UDC 669.017:539.16

MICROSTRUCTURE EVOLUTION AND DEUTERIUM TRAPPING IN LOW-ENERGY CASCADES AFTER IRRADIATION OF SS316 STAINLESS STEEL

S.A. Karpov, G.D. Tolstolutskaya, B.S. Sungurov, V.V. Ruzhytskiy
Institute of Solid State Physics, Material Science and Technology NSC KIPT, Kharkov, Ukraine
E-mail: karpofff@kipt.kharkov.ua

The release profile of deuterium from SS316 austenitic steel irradiated with low-energy deuterium ions was studied using thermal desorption spectroscopy as well as steel microstructure evolution after deuterium implantation and subsequent annealing by means of transmission electron microscopy. It was found that dislocation loops are predominant observed defects in SS316 steel irradiated to dose of ~ 1 dpa. The temperature range of deuterium retention is 300…600 K. Thermal desorption measurements show slightly-resolved stage of deuterium release with a maximum at temperature near 400 K. The energies of deuterium de-trapping have been analyzed using numerical simulations based on diffusion-trapping model.

INTRODUCTION

Stainless steels have a very broad field of application within industry due to its corrosion-resistant properties. The nuclear energy sector makes a lot of use of stainless steels.

Austenitic stainless steel of type SS316 is widely used as structural material in a reactor II and III generation due to its good creep resistance at high temperature and oxygen corrosion resistance [1]. This commercial grade has first been considered on the basis of it good industrial feedback, and have already been improved to perform reliably in the nuclear context. SS136 is considered for many components of future reactors worldwide, including sodium-cooled fast reactors, lead-cooled fast reactors, etc.

In structural materials of power plants during their operation condition there is an accumulation of gaseous impurities, in particular, helium and hydrogen that facilitate development of helium embrittlement, hydrogen embrittlement and swelling [2].

Because of a very low solubility of hydrogen isotopes in stainless steels, the presence of various lattice defects (vacancies, vacancy clusters, voids, dislocations, grain boundaries, impurities) strongly influences hydrogen isotope retention [3]. Therefore, parameters of trapping are essential for predicting hydrogen isotope transport in structural materials.

Due to the practical interest SS316 steel was extensively studied [4–7]. However, the need to create a new generation of power plants requires the solution of many problems of material science, in particular, studies of the combined effect of hydrogen and radiation-induced defects on materials.

Experimental investigations of the hydrogen-defect interaction are often performed by thermal desorption spectroscopy (TDS), and the parameters of the interaction are obtained by fitting numerical calculations based on diffusion-trapping codes to experimental thermal desorption spectra.

The goal of present paper is an investigation of ion implanted deuterium interaction with radiation-induced defects in SS316 austenitic stainless steel using TDS and TEM experimental techniques in conjunction with numerical calculations based on diffusion-trapping model as well as comparison of obtained data with those previously found for steels of type 18-10.

1. MATERIAL AND METHODS

The specimens were cut from a 130 μm thick hot-rolled SS316 steel foil and electrochemically polished with standard electrolyte. In order to de-gassing and to reduce the effect from pre-existing grain boundaries and dislocations, the steel was heat treated at 1050 °C for 10 min in target chamber in a vacuum ~10^{-4} Pa. Chemical composition of steel is shown in Table.

Chemical composition of SS316 steel, wt.%

C	Si	Mn	P	S	Cr	Ni	Mo	Fe
≤0.080	≤0.75	≤2.0	≤0.045	≤0.030	17.5	13.1	2.3	Bal.

The target chamber has a base pressure below $5 \cdot 10^{-5}$ Pa. A monopole mass-spectrometer is installed in the target chamber, which allows in situ TDS analysis.

The specimen with dimensions 27×7 mm is mounted on two electrical feedthroughs and can be resistively heated by AC current. Only a small central part (3 mm in diameter) of the sample is subjected to irradiation to minimize the influence of non-uniformity of the temperature over the sample surface during TDS. The sample temperature near the beam strike area is measured by a spot-welded chromel-alumel thermocouple.

The samples were implanted with 12 keV D_2 (6 keV/D) ions to the fluences in the range of $(1…3) \cdot 10^{20}$ D/m^2. The ion flux on the sample was in the range of $(1…2) \cdot 10^{18}$ D/(m^2·s). Ion implantation was performed at normal ion incidence, and the sample temperature did not exceed 300 K.

TDS experiments started within 15 min after the implantation was completed. The heating rate was 6 K/s.

Studies of the steel microstructure were performed by transmission electron microscopy at room temperature, employing standard bright-field techniques on an EM-125 electron microscope.

Preparation of specimens to suitable for TEM thickness was performed using standard jet

electropolishing from unirradiated surface. The initial structure of SS316 steel is shown in Fig. 1.

Fig. 1. The initial microstructure of SS316 steel after heat treatment at 1050 °C/0.5 h

The depth distribution of gas atoms concentration and damage was calculated by SRIM 2008 [8] and shown in Fig. 2. The damage calculations were performed with a displacement energy of 40 eV for Fe and Cr, as recommended in ASTM E521-96 (2009) [9].

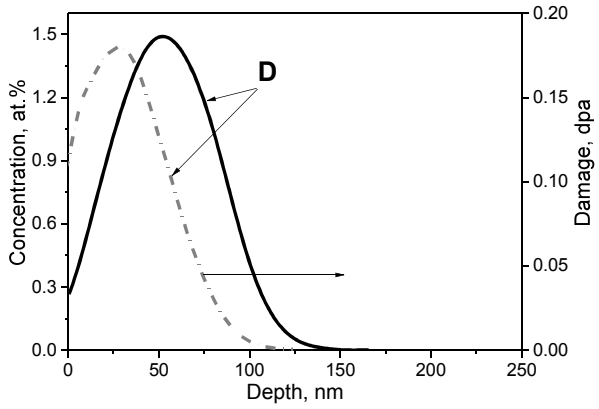

Fig. 2. Calculated 6 keV deuterium profiles of damage and concentration for $1 \cdot 10^{16}$ cm^{-2} irradiation dose

SRIM calculations have demonstrated that the damage profile is located within the depth of 0-100 nm, and maximum damage level of 0.18 dpa corresponds approximately to the distance of 26 nm from irradiated surface.

Since all the experiments were carried out in high vacuum conditions without exposure of the sample to air between implantation and TDS measurements, adsorption of impurities (like oxygen and carbon) on the sample surface was strongly reduced. Consequently, it is assumed that under the present experimental conditions the concentration of impurities on the sample surface was low, thus, the recombination rate was high enough not to affect the TDS spectra.

2. RESULTS AND DISCUSSION

The thermal desorption analysis was employed to observe hydrogen trapping and de-trapping behavior.

Fig. 3 shows TDS spectra from sample implanted to a fluence of $1 \cdot 10^{16}$ D^+/cm^2. The spectra consist of two poorly resolved peaks: around 385 K and around 425 K. The first rather high peak near 385 K is suggested to be composed of several narrower peaks also. In the investigated dose range $(1…3) \cdot 10^{16}$ cm^{-2} the amplitude of thermal desorption peaks increases virtually proportional to the radiation fluence. This indicates the deuterium trapping by defects of irradiation origin.

Previous studies of the interaction of ion-implanted hydrogen isotopes with radiation-induced defects in austenitic stainless steels have shown that the gas atoms quickly migrate in material bulk, their binding energy with defects characterized by low values, and after annealing to temperatures of 600 K almost all hydrogen atoms leave the implanted layer [10]. Present TDS measurements have shown the same tendency.

In order to deduce the deuterium trapping parameters, we have modeled the implantation, diffusion, trapping, de-trapping, and recombination processes that occur during the experiment. The modeling calculation is a numerical solution for the diffusion of deuterium in the presence of trapping sites (1), (2) and has been discussed in detail elsewhere [11].

$$\frac{\partial C(x,t)}{\partial t} = D(T)\frac{\partial^2 C(x,t)}{\partial x^2} - \sum_k S_k(x,t) + \varphi(x), \quad (1)$$

$$\frac{\partial G_k(x,t)}{\partial t} = S_k(x,t), \quad (2)$$

where C – concentration of hydrogen into solution; G_k – concentration of hydrogen in traps of k-type; S_k – the rate of the hydrogen concentration change in the defects of k-type; $\varphi(x)$ – the distribution of the hydrogen introduction rate through the depth; $D(T) = D_o \exp(-E_m/k_B T)$ – deuterium diffusivity.

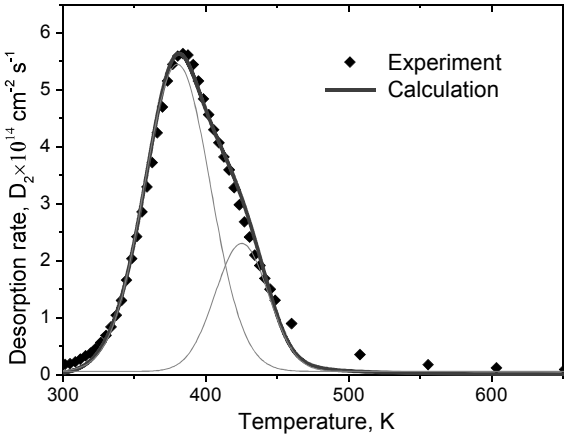

Fig. 3. The deuterium desorption spectra from SS316 steel, irradiated at T = 290 K to a dose of $1 \cdot 10^{16}$ D^+/cm^2 and calculated TDS profile using diffusion-trapping model

The presence of two desorption stages in the experimental spectra implies the consideration of (at least) two types of traps in the model.

It should be noted that in our calculations, as well as similar software packages [12, 13], it is assumed that the traps of gas atoms are represented as a distribution profile of a 1-dimensional defects of one or more types. The configuration of these distributions is often defined on the basis of calculated SRIM damage profiles for specified ion energy. Furthermore, each trap type can in general case to attach from the one to several hydrogen atoms.

The common issue of TDS experiments is the interpretation of the types of defects responsible for

particular peaks. In the case of irradiation of metals by light ions with energies in the keV range, mainly point defects are formed as the energy transfer from an incident ion to a metal atom is relatively low. We can assume that the two stages of deuterium desorption in the spectra shown in Fig. 3 correspond to the deuterium escaping from these traps.

Calculations performed on the assumption of no more than one hydrogen atom per trap, have good agreement with experimental TDS profile and provide the binding energies of 0.22 and 0.39 eV for low- and high-temperature desorption stage, respectively; while, the total concentration of defects exceeds a few atomic percent. This is contrary to current concepts [14] that the saturation level of Frenkel pairs in the volume of irradiated fcc metals is less than 1 at.%. Therefore, such approach to identification of traps as point defects seems to be unacceptable, that enforces to take into consideration another possible defect types and to involve the concept of multiple population of traps with deuterium atoms.

It should be noted that at room temperature irradiation the mobility of vacancies is low, so the fraction of vacancy clusters is small. Therefore, these defects were not included in the consideration.

Self-interstitials formed during irradiation due to their high mobility in austenite at room temperature can either disappear on the surface (since the ion range is relatively small) or agglomerate to form dislocation loops [15].

The defects of dislocation type are often regarded by researchers as possible trapping sites of hydrogen isotopes in metals. In particular, Ono [16] for Fe–9Cr–2W ferritic alloy clearly demonstrated deep correlation between the TDS of deuterium gas and dislocation loop annihilation. According to [16], deuterium ions irradiated on the specimen were trapped at dislocation loops and affects their thermal stability.

In the present study TEM observations have been employed to investigate steel microstructure evolution after deuterium implantation and subsequent annealing and its relation to gas release kinetics (Fig. 4).

TEM results show that implantation of deuterium in SS316 steel is accompanied by the creation of dislocation type defects. System of dislocation loops have been observed within the depth layer corresponding approximately to the ions range.

Nevertheless, as seen from Fig. 4, microstructure remains almost unchanged throughout the temperature range where the gas desorption process is observed. The coalescence of dislocation loops starts at annealing temperatures about 1000 K and definitively disappeared at ~ 1200 K. Consequently, the presence of radiation-induced dislocations in steel and thermally activated release of deuterium do not exhibit a distinct correlation.

Our previous detailed studies of 18-10 type steels [10] had showed that dislocation type defects are not effective traps for hydrogen isotopes in austenitic stainless steels. Besides, according to [17, 18], the binding energy of hydrogen with dislocation-type defects in stainless steels is 0.05...0.15 eV, and therefore, dislocations do not considerably affect the deuterium trapping in stainless steels at room temperature.

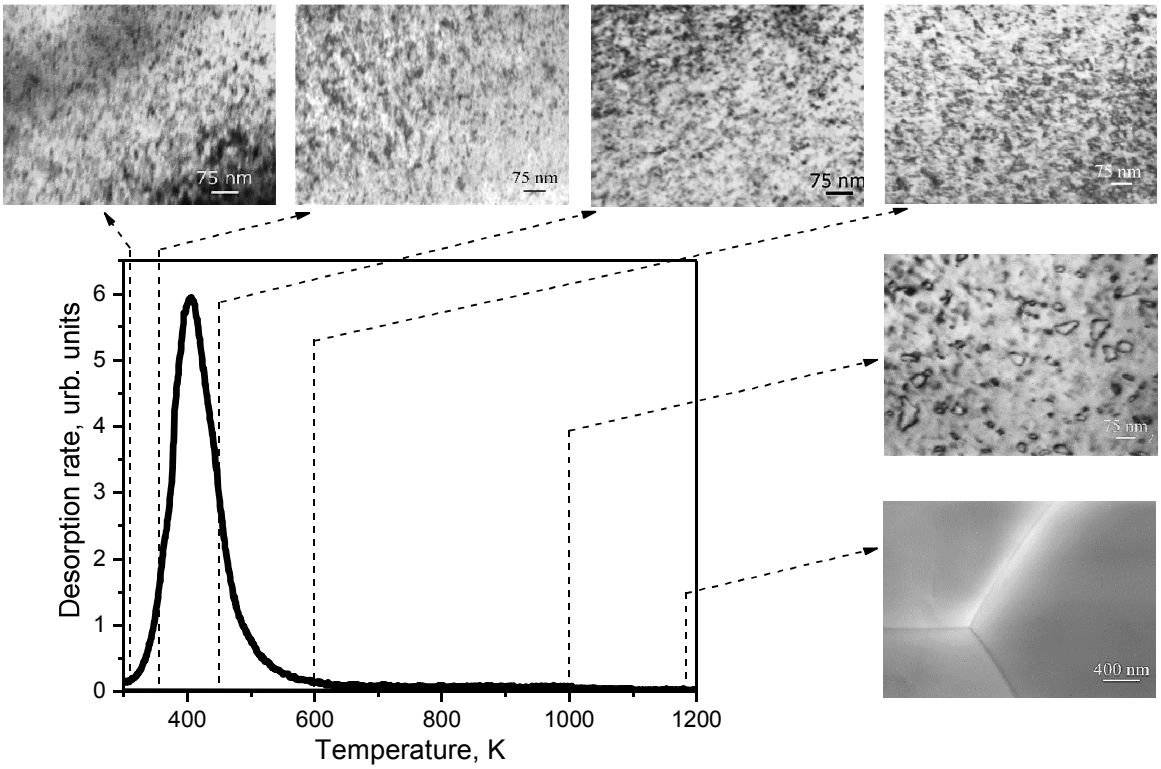

Fig. 4. Microstructure evolution and deuterium thermal desorption from SS316 steel, irradiated to a dose of $3 \cdot 10^{20}$ $D^+ \cdot m^{-2}$

Among the variety of possible defects, the concept of multiple capturing of deuterium atoms has developed most extensively with respect to vacancy type defects.

It may be suggested that multiple population of mono-vacancies with deuterium atoms can give a contribution to the desorption spectra in SS316 steel. According to theoretical predictions [19], the binding energies of the first and the second deuterium atom in a single vacancy are almost equal, whereas for the third and subsequent atoms they are considerably lower. As a result, the 425 K peak may be composed of two closely located peaks corresponding to the release of the first and the second trapped deuterium atom from a vacancy. Consequently, the 385 K peak will represent the superposition of a series of closely disposed peaks reflecting the de-trapping of the third and further deuterium atoms from a vacancy.

For simplicity, we have performed calculations that provide capturing of the one deuterium atom per trap for high-temperature stage of desorption and up to six deuterium atoms per trap for low-temperature peak. The result of calculations is shown in Fig. 3, and the obtained binding energies are (0.28±0.04) eV and (0.39±0.06) eV, for 385 and 425 K peaks, respectively.

According to our previous results, the calculated values of binding energies are virtually the same that were obtained for the case of deuterium irradiation of 18-10 type steels [10]. The value of 0.39 eV is in a good agreement with the value of binding energy of hydrogen with mono-vacancy in fcc metals. The total concentration of defects in such manner of calculation do not exceed 1 at.%.

Based on the these results, we suppose that the most preferred trapping sites of deuterium atoms in investigated SS316 austenitic stainless steel are vacancy type defects.

In addition, although the influence of dislocation loops seems insignificant, we have performed additional calculations involving these defects. Numerical simulations indicate that their presence does not affect the determined values of binding energies, and practically do not change deuterium transport in the material.

CONCLUSIONS

Interaction of ion implanted deuterium with SS316 austenitic stainless steel was studied by means of thermal desorption spectrometry and transmission electron microscopy. TDS profile was analyzed in the framework of diffusion-trapping model. The main results obtained are as follows:

1. The ion-implanted deuterium is weakly trapped by defects produced in low-energy displacement cascades. The temperature range of deuterium release is 300…600 K.

2. Irradiation of SS316 steel resulted in the formation of high density dislocation loops which are thermally stable up to 1000 K and have no considerable effect on deuterium transport in the material at room temperature.

3. According to calculations, most preferred trapping sites for deuterium atoms in investigated steel are vacancy type defects.

4. The observed data are consistent with those previously obtained for steels of type 18-10.

REFERENCES

1. S.J. Zinkle, G.S. Was. Materials challenges in nuclear energy // *Acta Mater.* 2013, v. 61, p. 735-758.

2. T. Tanaka, K. Oka, S. Ohnuki, S. Yamashita, T. Suda, S. Watanabe, E. Wakai. Synergistic effect of helium and hydrogen for defect evolution under multi-ion irradiation of Fe–Cr ferritic alloys // *J. Nucl. Mater.* 2004, v. 329-333, p. 294-298.

3. F.A. Garner, E.P. Simonen, B.M. Oliver, L.R. Greenwood, M.L. Grossbeck, W.G. Wolfer, P.M. Scott. Retention of hydrogen in fcc metals irradiated at temperatures leading to high densities of bubbles or voids // *J. Nucl. Mater.* 2006, v. 356, p. 122-135.

4. K.L. Wilson, M.I. Baskes. Deuterium trapping in irradiated 316 stainless steel // *J. Nucl. Mater.* 1978, v. 76/77, p. 291-297.

5. L. Fournier, B.H. Sencer, G.S. Was, et al. The influence of oversized solute additions on radiation-induced changes and post-irradiation intergranular stress corrosion cracking behavior in high-purity 316 stainless steels // *J. Nucl. Mater.* 2003, v. 321, N 2/3, p. 192-209.

6. T. Hirabayashi, M. Saeki, and E. Tachikawa. Effect of surface treatment on the sorption of tritium on type-316 stainless steel // *J. Nucl. Mater.* 1985, v. 127, p. 187-192.

7. Z. Kerner, A. Horvath, G. Nagy. Comparative electrochemical study of 08H18N10T, AISI304 and AISI316L stainless steels // *Electrochim. Acta.* 2007, v. 52, p. 7529-7537.

8. www.srim.org.

9. R.E. Stoller, M.B. Toloczko, G.S. Was, A.G. Certain, S. Dwaraknath, F.A. Garner. On the use of SRIM for computing radiation damage exposure // *Nucl. Instr. Methods Phys. Res. B.* 2013, v. 310, p. 75-80.

10. С.А. Карпов, В.В. Ружицкий, И.М. Неклюдов, В.И. Бендиков, Г.Д. Толстолуцкая. Параметры захвата и термоактивированного выхода дейтерия, ионно-имплантированного в сталь Х18Н10Т // *Металлофизика и новейшие технологии.* 2004, №12, с. 1661-1670.

11. В.И. Бендиков, С.А. Карпов, В.В. Ружицкий. *Численное моделирование термодесорбционных спектров водорода, имплантированного в металлы:* Препринт ХФТИ. Харьков: ННЦ ХФТИ, 2003, 16 с.

12. M.I. Baskes. *DIFFUSE 83*: Sandia, National Laboratories Report SAND83-8231, 1983.

13. G.R. Longhurst, D.F. Holland, J.L. Jones, B.J. Merrill. *TMAP4 User's Manual:* Idaho National Engineering Laboratory. EGG-FSP-10315. 1992.

14. R.C. Birtcher, R.S. Averback, T.H. Blewitt. Saturation behavior of cascade damage production using fission fragment and ion irradiations // *J. Nucl. Mater.* 1978, v. 75, N 1, p. 167-176.

15. R. Sakamoto, T. Muroga, N. Yoshida. Microstructural evolution induced by low energy hydrogen ion irradiation in tungsten // *J. Nucl. Mater.* 1995, v. 220-222, p. 819-822.

16. K. Ono, M. Miyamoto, K. Arakawa, S. Matsumoto, F. Kudo. Effects of precipitated helium, deuterium or alloy elements on glissile motion of dislocation loops in Fe-9Cr-2W ferritic alloy // *J. Nucl. Mater.* 2014, v. 455, N 1-3, p. 162-166.

17. A. Atrens, N.F. Fiore, K. Miura. Dislocation damping and hydrogen pinning in austenitic stainless steels // *J. Appl. Phys.* 1977, v. 48, N 10, p. 4247-4251.

18. A. Atrens, N.F. Fiore, K. Miura. Dislocation damping and hydrogen pinning in austenitic stainless steels // *J. Appl. Phys.* 1977, v. 48, N 10, p. 4247-4251.

19. S.M. Myers, P. Nordlander, F. Besenbacher, et al. Theoretical examination of the trapping of ion-implanted hydrogen in metals // *Phys. Rev. B.* 1986, v. 33, N 2, p. 854-863.

Article received 03.03.2017

ЭВОЛЮЦИЯ МИКРОСТРУКТУРЫ И ЗАХВАТ ДЕЙТЕРИЯ ПРИ НИЗКОЭНЕРГЕТИЧЕСКОМ ОБЛУЧЕНИИ АУСТЕНИТНОЙ НЕРЖАВЕЮЩЕЙ СТАЛИ SS316

С.А. Карпов, Г.Д. Толстолуцкая, Б.С. Сунгуров, В.В. Ружицкий

Методом термодесорбционной масс-спектроскопии изучено термоактивированное выделение дейтерия из аустенитной нержавеющей стали SS316, облученной низкоэнергетическими ионами дейтерия, а также исследована эволюция микроструктуры стали после имплантации дейтерия и последующих отжигов с помощью просвечивающей электронной микроскопии. Было установлено, что облучение до дозы ~ 1 сна приводит к образованию дислокационных петель. Температурный интервал удержания дейтерия составляет 300…600 К. Измерения показали наличие одной слаборазрешимой стадии выхода дейтерия с максимумом при температуре ~ 400 К. Выполнен анализ энергии связи дейтерия с ловушками по кривым термодесорбции с помощью численного моделирования, основанного на модели диффузии атомов газа в поле радиационных дефектов.

ЕВОЛЮЦІЯ МІКРОСТРУКТУРИ І ЗАХОПЛЕННЯ ДЕЙТЕРІЮ ПРИ НИЗЬКОЕНЕРГЕТИЧНОМУ ОПРОМІНЮВАННІ АУСТЕНІТНОЇ НЕРЖАВІЮЧОЇ СТАЛІ SS316

С.О. Карпов, Г.Д. Толстолуцька, Б.С. Сунгуров, В.В. Ружицький

Методом термодесорбційної мас-спектроскопії вивчено термоактивоване виділення дейтерію з аустенітної нержавіючої сталі SS316, опроміненої низькоенергетичними іонами дейтерію, а також досліджено еволюцію мікроструктури сталі після імплантації дейтерію і наступних відпалів за допомогою просвічувальної електронної мікроскопії. Було встановлено, що опромінення до дози ~ 1 зна призводить до утворення дислокаційних петель. Температурний інтервал утримання дейтерію становить 300…600 К. Вимірювання показали наявність однієї слабовирішуваною стадії виходу дейтерію з максимумом при температурі ~ 400 К. Проаналізовано енергії зв'язку дейтерію з пастками по кривим термодесорбції за допомогою чисельного моделювання, заснованого на моделі дифузії атомів газу в полі радіаційних дефектів.